Catalysis Communications 48 (2014) 50–54

Contents lists available at ScienceDirect

Catalysis Communications

journal homepage: www.elsevier.com/locate/catcom

Short Communication

Catalytic abatement of CO over highly stable Pt supported on Ta_2O_5 nanotubes

Renato V. Gonçalves [a,*], Robert Wojcieszak [a], Paula M. Uberman [a], Dario Eberhardt [b], Erico Teixeira-Neto [c], Sergio Ribeiro Teixeira [b], Liane M. Rossi [a,*]

[a] Laboratory of Nanomaterials & Catalysis, Institute of Chemistry, USP, Av. Professor Lineu Prestes, 748, São Paulo 05508-000, SP, Brazil
[b] Institute of Physics, UFRGS, Av. Bento Gonçalves 9500, Porto Alegre, P.O. Box 15051, Rio Grande do Sul, RS, Brazil
[c] Laboratory of Analytical Electron Microscopy, Institute of Chemistry, USP, Av. Professor Lineu Prestes, 748, São Paulo 05508-000, SP, Brazil

ARTICLE INFO

Article history:
Received 18 December 2013
Received in revised form 20 January 2014
Accepted 22 January 2014
Available online 31 January 2014

Keywords:
CO oxidation
Pt nanoparticles
Ta_2O_5 nanotubes
Sputtering deposition

ABSTRACT

The development of active and stable catalysts has emerged as an important strategy in the catalytic abatement of CO. This article reports the use of the novel Pt-based catalyst supported on crystalline Ta_2O_5 nanotubes prepared by sputtering and anodization methods in CO oxidation reaction. Crystalline and amorphous Ta_2O_5 NTs and Pt modified sample were found active in low temperature CO oxidation. Results showed that active and highly stable Pt/Ta_2O_5 NTs catalyst could be a promising system for CO removal from gas exhaust.

1. Introduction

There is no perfect energy source that has no environmental impact. Nowadays, even with the best regulation concerning air pollution, industrial production cannot be done with any impact on the environment. Moreover, yet, no form of energy production can meet those standards. One of the most dangerous gas pollution is the CO emission. The largest contribution in CO emission is coming from motor vehicles. Especially in urban area this contribution can exceed 90% which turns the catalytic removal of CO as one of the most important application area in both industrial and automotive pollution control [1–4]. Over the last 20 years, the development of highly active catalysts for the catalytic oxidation of carbon monoxide has attracted much attention. An important application is the preferential oxidation of CO (PROX) in the presence of H_2 for the removal of CO traces from H_2 in proton exchange membrane (PEM) fuel cells [5,6]. In the absence of carbon monoxide these fuel cells are able to run at lower temperatures with an enhanced efficiency. Pt supported on Al_2O_3, CeO_2 [7] or Fe_2O_3 [8] showed improved performance for CO oxidation compared with the unsupported catalysts. The use of semiconductor oxides, such as TiO_2, as catalyst support for metallic NPs has emerged as an important strategy to increase their catalytic activities for CO oxidation [9–12]. Recently, Somorjai et al. found a strong correlation between the oxidation state of the oxide support and the catalytic activity at the oxide–Pt interface [8].

Tantalum pentoxide (Ta_2O_5) is a functional semiconductor oxide material widely used as a gas sensor, hot mirror coating, waveguide and photocatalyst [13,14]. However, to the best of our knowledge, Ta_2O_5 nanotubes has not yet been studied as a support for noble metal NPs (e.g., Pt, Pd, Au) in the CO oxidation reaction. The structural defects and vacancies present on the surface of Ta_2O_5 can provide enhanced rates of the diffusion of adsorbed oxygen and lead to an increase in the catalytic activity [15–17].

Recently, a modified sputtering deposition method has been employed to deposit Ni and Pd NPs directly on the surface of the solid supports [18,19]. The sputtering method has several advantages when compared to the classical bottom-up methods for the preparation of metal NPs, including no contamination from solvents or precursors, direct deposition on both liquid and solid supports, and synthesis of large amounts of NPs by the simple control of physical parameters (power and time) [20–22].

Herein, a modified sputtering deposition method [18] was chosen to produce Pt NPs directly onto Ta_2O_5 NT support. Ta_2O_5 NT support was successfully prepared by anodization method [23]. The catalytic activity of Pt NPs supported on Ta_2O_5 NTs was studied for the oxidation of carbon monoxide.

2. Experimental

2.1. Synthesis of Ta_2O_5 NTs

Ta_2O_5 nanotubes were prepared by anodizing high-purity Ta disks (3 cm of diameter, 99.99%) in an electrolyte contained 1 vol.% of

* Corresponding authors.
E-mail addresses: rsvg12@iq.usp.br (R.V. Gonçalves), lrossi@iq.usp.br (L.M. Rossi).

1566-7367/$ – see front matter © 2014 Elsevier B.V. All rights reserved.
http://dx.doi.org/10.1016/j.catcom.2014.01.020

hydrofluoride acid (HF, 40%), 4 vol.% deionised water, and sulfuric acid (H_2SO_4, 98%) as the solvent at a voltage of 50 V at 50 °C for 20 min [23]. After the anodization process the as-prepared NTs were calcined in a muffle furnace under atmospheric air at 800 °C for 60 min, with a heating rate of 5 °C min^{-1}.

2.2. Preparation of platinum nanoparticle

Platinum nanoparticles were prepared by sputtering method. A Pt target was sputter deposited onto Ta_2O_5 NT surface by using a mechanical agitation apparatus, placed inside the vacuum chamber, to permit homogenous distribution of the obtained Pt NPs on the NTs [18], (scheme S1). For more details of Pt NPs preparation by sputtering method, readers are encouraged to see Supporting Information.

2.3. Characterizations

A scanning electron microscope (FESEM, FEI Inspect F50 — LNNano), transmission electron microscope (JEOL JEM 2100F — LNNano) and a high-resolution transmission electron microscope (HRTEM, model JEOL JEM 3010 — LNNano) were used to observe the morphologies of the Ta_2O_5 NTs and Pt NPs, respectively. X-ray powder diffraction (XRD) was applied to analyze crystal structures. The diffraction patterns were recorded in a Philips X'PERT diffractometer with Cu Kα radiation (λ = 1.54 Å) at 2theta = 5–100° with a 0.02° step size and measuring time of 5 s per step. Rietveld refinement procedures were used for the crystal structure analyses using Fullprof software [24]. Measurements of specific surface area (S_{BET}) were calculated according to the Brunauer–Emmett–Teller method (BET) using nitrogen absorption isotherms obtained in a Micromeritics TriStar II 3020 apparatus. X-ray photoelectron spectroscopy (XPS) was applied to analyze chemical composition of the Ta_2O_5 NTs using conventional equipment with a high-performance hemispheric SPECSLAB II energy analyzer and a non-monochromatic Al Kα (hν = 1486.6 eV) radiation as the excitation source.

2.4. Catalytic CO oxidation

The catalytic CO oxidation experiments were performed using 20 mg of Ta_2O_5 NTs powder placed in a quartz tube reactor (length: 20 mm, width: 5 mm). The reaction temperature was controlled by a temperature sensor on the Integrated Microreactor-MS with CATLAB-PCS Module & QIC-20 MS. A continuous flow of the reactant mixture containing 1.75 vol.% CO, 7 vol.% O_2, and Ar balance was passed through the reactor with a total flow rate of 100 mL min^{-1}.

3. Results and discussion

Ta_2O_5 NTs were obtained after the Ta metal was anodized for 20 min in H_2SO_4-based electrolytes [23]. As-anodized Ta_2O_5 NTs were amorphous and thermal treatment process was performed to achieve its crystallization. Here, the Ta_2O_5 NTs were calcined at 800 °C for 60 min in a conventional furnace and their structural properties were examined by means of X-ray diffraction (Cu-Kα radiation). The XRD patterns along with Rietveld refined data, is presented in Fig. 1, revealed that the amorphous NTs were converted to an orthorhombic phase (JPCDS file 25-0922). Rietveld refinements show that the refined cell parameters are a = 6.20, b = 40.28 and c = 3.88 Å and that the crystal size of the Ta_2O_5 NTs is about 15.5 nm with a preferred orientation in the (0 0 1) direction. By the XRD pattern, the Ta_2O_5 sample calcined at 800 °C at 60 min showed a degree of crystallinity of the 34% (more details see Supporting Information).

The morphologies of the Ta_2O_5 NTs were characterized by field-emission scanning electron microscopy (FESEM, FEI Inspect F50) and scanning transmission electron microscopy (STEM JEOL JEM 2100F). As anodized Ta_2O_5 NTs measured about 5 μm in length, 100 nm in diameter, 50 nm in pore diameter and with the wall thickness of about 30 nm, (Fig. 2). As anodized NTs have continuous smooth walls and are open at the top. The inset in Fig. 2b is a bottom view of the Ta_2O_5 NTs after calcination, indicating that the NTs are closed at the bottom. After calcination at 800 °C for 60 min, small holes and grains are observed in the NTs wall (Fig. 2c). However, the tubular structure was not yet affected [25]. Fig. 2d shows a HRTEM image of the Ta_2O_5 NTs support after the calcination. The inset in Fig. 2d corresponds to an interplanar distance of 0.389 nm, which are consistent with the interplanar distance of (0 0 1) planes of Ta_2O_5. The fringes confirm the crystallinity of the Ta_2O_5 NTs, which is in accordance with the corresponding fast Fourier transformation (FFT) shown in the inset (Fig. 2d).

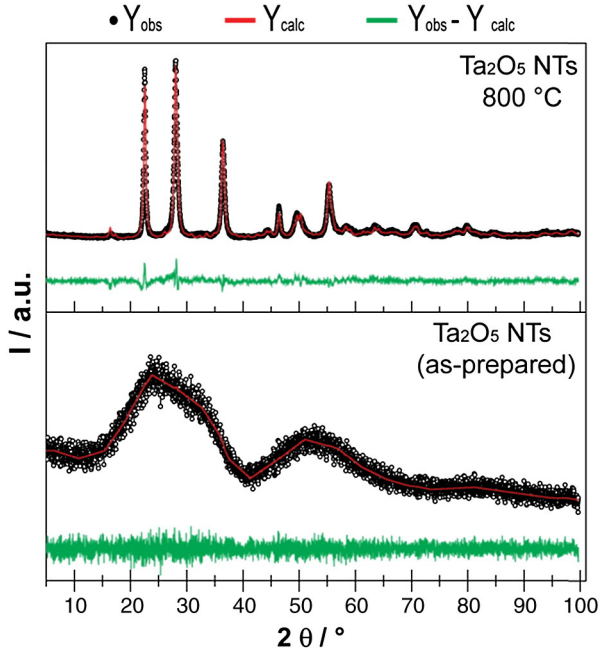

Fig. 1. XRD patterns for as-prepared and calcined Ta_2O_5 NTs.

The specific surface area (S_{BET}) of 16.2 and 19.8 m^2 g^{-1} was found for the as-anodized and calcined NTs at 800 for 60 min, respectively (Table 1). XPS spectroscopy was used to analyze the surface chemistry of the prepared NTs. The as-anodized NTs showed sulfur and fluorine contamination with a molecular concentration on the surface of about 6 and 5%, respectively (Table 1). These contaminants originated from HF and H_2SO_4 used in the preparation of Ta_2O_5 NTs. Both S and F were completely removed from the material surface by heating the NTs at 800 °C for 60 min.

Crystalline Ta_2O_5 NTs (800 °C for 60 min) were used as the support for the deposition of Pt NPs by a modified sputtering method shown in Scheme 1.

Fig. 2 shows the representative top-view STEM images of the Ta_2O_5 NTs after Pt NPs deposition. Higher magnification STEM image (Fig. 2e), shows Pt NPs of 2–1.7 nm in size on Ta_2O_5 NTs. STEM image obtained using a HAADF detector confirms the presence of these very small Pt NPs by atomic number contrast between the Pt and Ta_2O_5 (Fig. 2f and g). During the sputtering process, it is expected that majority of the formed Pt NPs will be on the external surface of NTs. As nanotubes have a large diameter (50 nm) compared to the diameter of the nanoparticles, it is possible also that nanoparticles could be deposited inside the nanotubes. However this probability is rather small.

The Pt loading of 0.57 wt.% was quantified using flame atomic absorption spectroscopy (FAAS). The optical images (see Scheme 1) show the color evolution (from white to gray) of the material before and after Pt sputtering, which confirms the deposition of metallic Pt.

In the first set of experiments, the catalytic activity of the Ta_2O_5 supports (crystalline and amorphous Ta_2O_5 NTs) was investigated in the CO

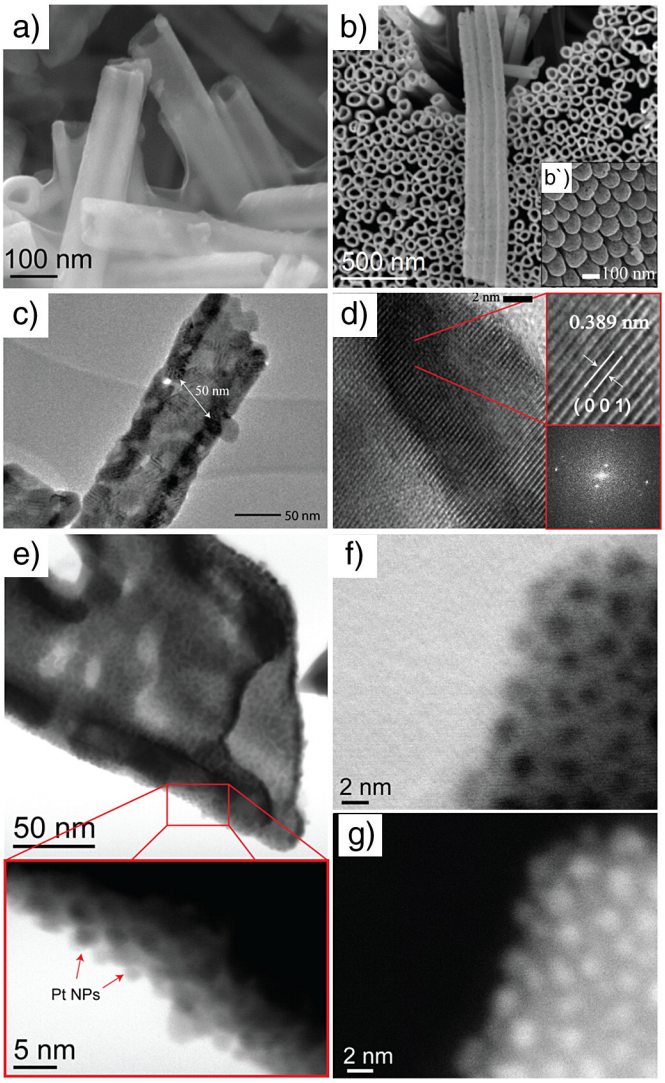

Fig. 2. FESEM images: a) as-prepared (amorphous) Ta_2O_5 NTs and b) crystalline Ta_2O_5 NTs; c) TEM image of crystalline Ta_2O_5 NTs, d) HRTEM image and the FFT pattern (inset) of crystalline Ta_2O_5 NTs, e) STEM image of crystalline Ta_2O_5 NTs uniformly loaded with Pt NPs, f) STEM image of high magnification of Pt NPs and g) HAADF-STEM image of Pt NPs.

oxidation reaction and results are presented in Table 2. The efficiency of Ta_2O_5 NTs in the carbon monoxide conversion was confirmed by a series of catalytic experiments and significant differences were observed in the catalytic activity of amorphous and crystalline NTs as described below. While, the amorphous material demonstrated initial conversion at 200 °C and reached the 100% conversion level at 438 °C, the CO oxidation over the crystalline Ta_2O_5 NTs started at about 157 °C and reached 100% conversion at 259 °C (Table 2). The T_{50} values (light-off temperature) for the CO oxidation reaction are quite low for both amorphous and crystalline samples at 313 and 249 °C, respectively. With the

Table 1
Characterization of the Ta_2O_5 NTs supports.

	Ta_2O_5 NTs (As-prepared)	Ta_2O_5 NTs (Crystalline)
Crystal structure	Amorphous	Orthorhombic
S_{BET}[a] ($m^2\ g^{-1}$)	16.4 ± 0.3	18.2 ± 0.4
S2p[b]	6%	Not detected-
F1s[b]	5%	Not detected-

[a] Specific surface area.
[b] Chemical surface composition (%) by XPS.

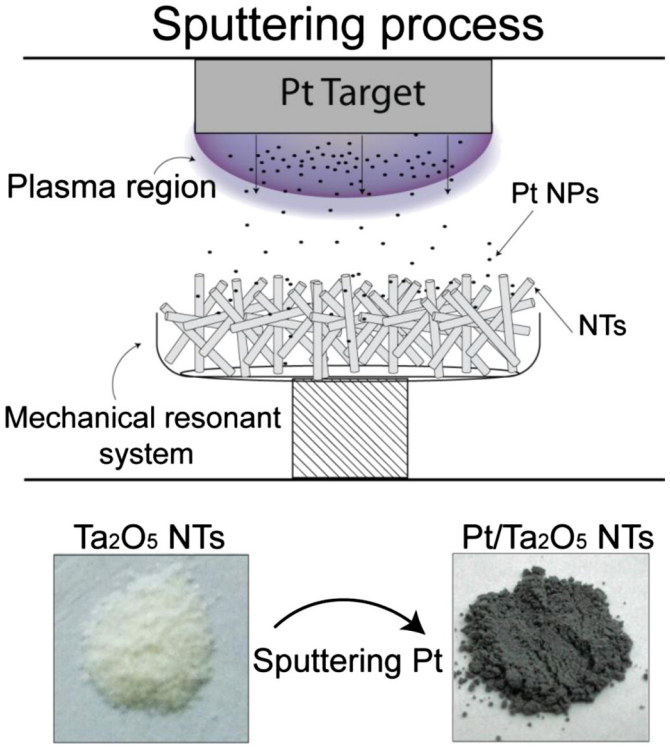

Scheme 1. Schematic representation of the Pt NPs deposition on Ta_2O_5 NTs support by the modified sputtering method and optical images of Ta_2O_5 NT powder before and after deposition of Pt NPs.

addition of Pt NPs on Ta_2O_5 NTs crystalline, the T_{50} value was significantly reduced (ΔT) to 151 °C (see Table 2).

The crystalline Ta_2O_5 NTs exhibited higher catalytic activity than the amorphous NTs, with any significant difference in the surface area of these materials (Table 1). This suggests that the high crystallinity of the calcined material plays an important role and strongly influenced the catalytic activity. The differences observed in chemical composition of the surface (presence of S and F in the case of amorphous material) also should be taking account. Indeed, some works stressed on the poisoning effect of chlorine contamination in CO oxidation reaction. Cl was found to act as a poison, making both the adsorption of O_2 and the formation of the CO–O_2 intermediate complexes more difficult [26–28]. Thereby, the crystalline Ta_2O_5 NTs seems to be a more promising support for Pt catalyst since this material demonstrated higher activity and no contaminations on the surface.

After the deposition of Pt NPs onto crystalline Ta_2O_5 NTs, the catalytic activity of the material in CO oxidation was further improved. In this case, the CO oxidation process started at low temperature (97 °C) and reached 100% conversion at 178 °C (Table 2). A clear indication of the increase of activity in the case of Pt/Ta_2O_5 catalyst was observed in the reaction rate expressed per catalyst mass at 200 °C. It was enhanced 24 and 37 times as compared to the crystalline and amorphous Ta_2O_5, respectively (Table 2). Additionally, Fig. 3a shows the CO conversion

Table 2
Catalytic activity of the Ta_2O_5 NTs supports and Pt/Ta_2O_5 in CO oxidation.

Sample	$T_{initial}$[a] (°C)	$T_{50\%}$[b] (°C)	$T_{100\%}$[c] (°C)	Rate[d]
Ta_2O_5 NTs (as-anodized)	200	313	438	0.09
Crystalline Ta_2O_5 NTs	157	249	259	0.14
Pt/Ta_2O_5 NTs	97	151	178	3.34

[a] Temperature of initial conversion.
[b] Temperature of 50% of CO conversion.
[c] Temperature of 100% of CO conversion.
[d] Reaction rate expressed in $mmol_{CO}\ g^{-1}\ s^{-1}$.

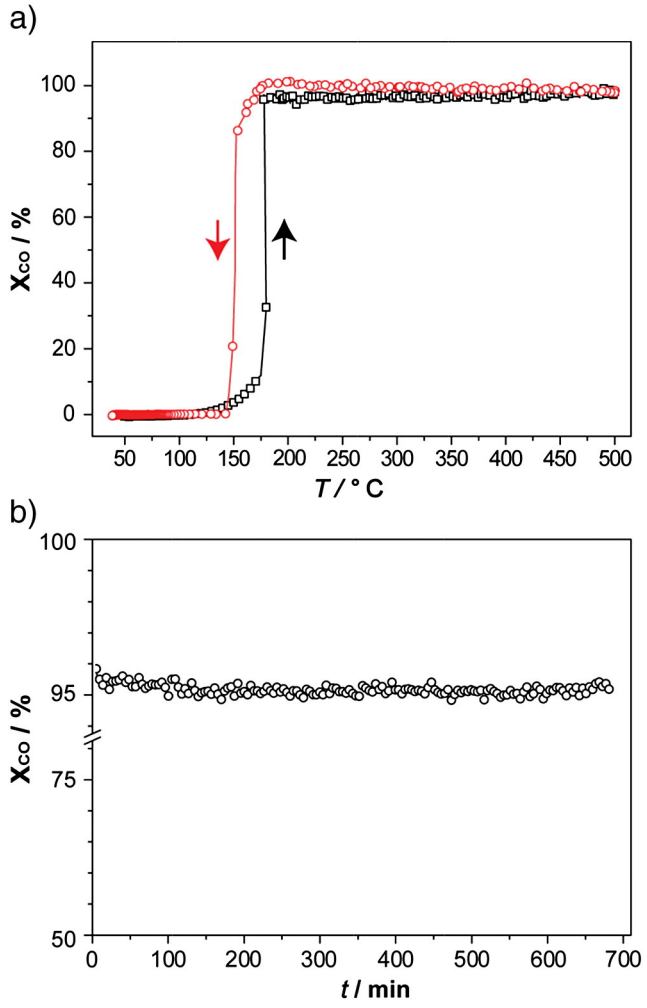

Fig. 3. a) CO conversion as a function of temperature over Pt/Ta_2O_5 NTs (black and red arrows indicate the reaction temperature increasing and decreasing, respectively) and b) Temporal stability of CO oxidation reaction versus time-on-stream over Pt/Ta_2O_5 NTs at 160 °C. (For interpretation of the references to color in this figure legend, the reader is referred to the web version of this article.)

curves for heating and cooling cycles using Pt NPs supported on crystalline Ta_2O_5 NTs without any pretreatment of the catalyst.

As shown in Fig. 3a, the CO conversion increased smoothly from room temperature to less than 175 °C; then, a sudden sharp jump to the maximum CO conversion (100%) occurred at 178 °C and was maintained until 500 °C. In the cooling cycle, a strong counterclockwise hysteresis in activity was observed, suggesting the activation of the catalyst in the heating cycle. The specific rate of the reaction expressed by mass of the Pt calculated at 10% of conversion is 60 mmol $CO \cdot s^{-1} \cdot g_{Pt}^{-1}$ (at 162 °C). This value is at least 100 times higher than other Pt catalysts reported in the literature [29,30].

One on the most important property of the catalyst is its resistance to poisoning, coke deposition or particle size growth. The stability of the Pt/Ta_2O_5 NTs catalyst was tested at 160 °C for long time-on-stream after the first catalytic cycle. As shown in Fig. 3b, high conversion of CO to CO_2 (96%) was maintained for 16 h without any loss of activity. This behavior confirms the very high stability of the Pt/Ta_2O_5 compared to other examples in the literature, such as the Pt/TiO_2 NTs catalyst which deactivated just after the first catalytic run [12,29].

Overall, the Pt/Ta_2O_5 catalyst studied here showed better stability and lower reaction temperatures for CO oxidation than Pt catalysts supported on other semiconductor supports such as TiO_2 [31], CeO_2 [7], and Nb_2O_5 [32]. The catalyst reached 100% conversion of CO, and this maximum activity could be traversed from both heating and cooling cycles without any loss of activity. This behavior excludes side reactions, coke deposition, and product inhibition as primary causes of catalyst deactivation.

4. Conclusions

In summary, crystalline Ta_2O_5 NTs prepared by anodization and calcination exhibited higher catalytic activity for CO oxidation than amorphous Ta_2O_5 NTs sample. Furthermore, the deposition of ultra-small Pt NPs prepared by a sputtering method improved the catalytic properties and reduced the reaction temperature to less than 200 °C. Moreover, this catalyst showed remarkable high stability as compared with other highly active Pt materials [12]. This is a very important and highly desirable property from a practical point of view.

Acknowledgments

The authors acknowledge CNPq, FAPESP, FAPERGS, and TWAS for the financial support. The authors also would like to thank the Electron Microscopy Laboratory (LME) of the Brazilian Nanotechnology National Laboratory (LNNano) for the use of their HRTEM, FESEM and TEM-FEG facility.

Appendix A. Supplementary data

Supplementary data to this article can be found online at http://dx.doi.org/10.1016/j.catcom.2014.01.020.

References

[1] S. Royer, D. Duprez, Catalytic oxidation of carbon monoxide over transition metal oxides, ChemCatChem 3 (2011) 24–65.
[2] G.C. Bond, D.T. Thompson, Catalysis by gold, Catal. Rev. 41 (1999) 319–388.
[3] N.M. Marković, P.N. Ross Jr., Surface science studies of model fuel cell electrocatalysts, Surf. Sci. Rep. 45 (2002) 117–229.
[4] M.J. Kahlich, H.A. Gasteiger, R.J. Behm, Kinetics of the selective CO oxidation in H2-rich gas on Pt/Al2O3, J. Catal. 171 (1997) 93–105.
[5] E.D. Park, D. Lee, H.C. Lee, Recent progress in selective CO removal in a H-2-rich stream, Catal. Today 139 (2009) 280–290.
[6] H.F. Oetjen, V.M. Schmidt, U. Stimming, F. Trila, Performance data of a proton exchange membrane fuel cell using H-2/CO as fuel gas, J. Electrochem. Soc. 143 (1996) 3838–3842.
[7] A. Holmgren, B. Andersson, D. Duprez, Interactions of CO with Pt/ceria catalysts, Appl. Catal. B Environ. 22 (1999) 215–230.
[8] K. An, S. Alayoglu, N. Musselwhite, S. Plamthottam, G. Melaet, A.E. Lindeman, G.A. Somorjai, Enhanced CO oxidation rates at the interface of mesoporous oxides and Pt nanoparticles, J. Am. Chem. Soc. 135 (2013) 16689–16696.
[9] Y. Watanabe, X. Wu, H. Hirata, N. Isomura, Size-dependent catalytic activity and geometries of size-selected Pt clusters on TiO 2(110) surfaces, Catal. Sci. Technol. 1 (2011) 1490–1495.
[10] K. Grass, H.G. Lintz, The kinetics of carbon monoxide oxidation on tin(IV) oxide supported platinum catalysts, J. Catal. 172 (1997) 446–452.
[11] C. Becker, C.R. Henry, Cluster size dependent kinetics for the oxidation of CO on a Pd/MgO(100) model catalyst, Surf. Sci. 352–354 (1996) 457–462.
[12] A.V. Grigorieva, E.A. Goodilin, L.E. Derlyukova, T.A. Anufrieva, A.B. Tarasov, Y.A. Dobrovolskii, Y.D. Tretyakov, Titania nanotubes supported platinum catalyst in CO oxidation process, Appl. Catal. A Gen. 362 (2009) 20–25.
[13] C. Christensen, R. de Reus, S. Bouwstra, Tantalum oxide thin films as protective coatings for sensors, J. Micromech. Microeng. 9 (1999) 113–118.
[14] C. Chaneliere, J.L. Autran, R.A.B. Devine, B. Balland, Tantalum pentoxide (Ta2O5) thin films for advanced dielectric applications, Mater. Sci. Eng. R 22 (1998) 269–322.
[15] H. Sawada, K. Kawakami, Electronic structure of oxygen vacancy in Ta2O5, J. Appl. Phys. 86 (1999) 956–959.
[16] S.P. Garg, N. Krishnamurthy, A. Awasthi, M. Venkatraman, The O–Ta (oxygen–tantalum) system, J. Phase Equilib. 17 (1996) 63–77.
[17] K. Lehovec, Lattice structure of β-Ta2O5, J. Less. Common. Met. 7 (1964) 397–410.
[18] R. Bussamara, D. Eberhardt, A.F. Feil, P. Migowski, H. Wender, D.P. de Moraes, G. Machado, R.M. Papaleo, S.R. Teixeira, J. Dupont, Sputtering deposition of magnetic Ni nanoparticles directly onto an enzyme surface: a novel method to obtain a magnetic biocatalyst, Chem. Commun. 49 (2013) 1273–1275.
[19] L. Luza, A. Gual, D. Eberhardt, S.R. Teixeira, S.S.X. Chiaro, J. Dupont, "Imprinting" catalytically active Pd nanoparticles onto ionic-liquid-modified Al2O3 supports, ChemCatChem 5 (2013) 2471–2478.
[20] J.A. Thornton, Influence of apparatus geometry and deposition conditions on the structure and topography of thick sputtered coatings, J. Vac. Sci. Technol. 11 (1974) 666–670.

[21] H. Wender, R.V. Goncalves, A.F. Feil, P. Migowski, F.S. Poletto, A.R. Pohlmann, J. Dupont, S.R. Teixeira, Sputtering onto liquids: from thin films to nanoparticles, J. Phys. Chem. C 115 (2011) 16362–16367.
[22] H. Wender, P. Migowski, A.F. Feil, S.R. Teixeira, J. Dupont, Sputtering deposition of nanoparticles onto liquid substrates: recent advances and future trends, Coord. Chem. Rev. 257 (2013) 2468–2483.
[23] R.V. Gonçalves, P. Migowski, H. Wender, D. Eberhardt, D.E. Weibel, F.v.C. Sonaglio, M.J.M. Zapata, J. Dupont, A.F. Feil, S.R. Teixeira, Ta2O5 nanotubes obtained by anodization: effect of thermal treatment on the photocatalytic activity for hydrogen production, J. Phys. Chem. C 116 (2012) 14022–14030.
[24] J. Rodriguezcarvajal, Recent advances in magnetic-structure determination by neutron powder diffraction, Physica B 192 (1993) 55–69.
[25] R.V. Goncalves, P. Migowski, H. Wender, A.F. Feil, M.J.M. Zapata, S. jadoon, F. Bernardi, G. Azevedo, S.R. Teixeira, On the crystallization of Ta2O5 nanotubes: structural and local atomic properties investigated by EXAFS and XRD, CrystEngComm 16 (2014) 797–804.
[26] H.S. Oh, J.H. Yang, C.K. Costello, Y.M. Wang, S.R. Bare, H.H. Kung, M.C. Kung, Selective catalytic oxidation of CO: effect of chloride on supported Au catalysts, J. Catal. 210 (2002) 375–386.
[27] P. Broqvist, L.M. Molina, H. Grönbeck, B. Hammer, Promoting and poisoning effects of Na and Cl coadsorption on CO oxidation over MgO-supported Au nanoparticles, J. Catal. 227 (2004) 217–226.
[28] C.K. Costello, M.C. Kung, H.S. Oh, Y. Wang, H.H. Kung, Nature of the active site for CO oxidation on highly active Au/γ-Al2O3, Appl. Catal. A Gen. 232 (2002) 159–168.
[29] L. Liu, F. Zhou, L. Wang, X. Qi, F. Shi, Y. Deng, Low-temperature CO oxidation over supported Pt, Pd catalysts: particular role of FeOx support for oxygen supply during reactions, J. Catal. 274 (2010) 1–10.
[30] G.R. Bamwenda, S. Tsubota, T. Nakamura, M. Haruta, The influence of the preparation methods on the catalytic activity of platinum and gold supported on TiO2 for CO oxidation, Catal. Lett. 44 (1997) 83–87.
[31] S. Bonanni, K. Aït-Mansour, H. Brune, W. Harbich, Overcoming the strong metal–support interaction state: CO oxidation on TiO2(110)-supported Pt nanoclusters, ACS Catal. 1 (2011) 385–389.
[32] P. Marques, N.F.P. Ribeiro, M. Schmal, D.A.G. Aranda, M.M.V.M. Souza, Selective CO oxidation in the presence of H2 over Pt and Pt–Sn catalysts supported on niobia, J. Power Sources 158 (2006) 504–508.